


## Article

# Influence of Turbulence Effects on the Runup of Tsunami Waves on the Shore within the Framework of the Navier–Stokes Equations

Andrey Kozelkov <sup>1,2</sup> , Elena Tyatyushkina <sup>1,2</sup>, Vadim Kurulin <sup>1,2</sup> and Andrey Kurkin <sup>2,\*</sup>

<sup>1</sup> Russian Federal Nuclear Center-All-Russian Research Institute of Experimental Physics, 607188 Nizhny Novgorod, Russia; askozelkov@mail.ru (A.K.); leno4ka-07@mail.ru (E.T.); kurulin@mail.ru (V.K.)

<sup>2</sup> Department of Applied Mathematics, Nizhny Novgorod State Technical University n.a. R.E. Alekseev, 603155 Nizhny Novgorod, Russia

\* Correspondence: aakurkin@nntu.ru

**Abstract:** This paper considers turbulence effects on tsunami runup on the shore in tsunami simulations using the system of three-dimensional Navier–Stokes equations. The turbulence effects in tsunami propagation and runup are studied by solving the problem of a wave propagating in a nonuniform-bottom pool and collapsing with a barrier. To solve this problem, we used the turbulence model, RANS SST (Reynolds-averaged Navier–Stokes shear stress transport). We compared the wave profiles at different times during wave propagation, runup, and collapse. To quantify the turbulence effects, we also compared the forces acting on the basin bottom. We demonstrated that the turbulence had almost no effect on the shape of the wave and the way of its propagation (except collapse). However, turbulence effects during the runup and collapse became noticeable and could boost the flow (increasing the pressure force and the total force) by up to 25 percent.

**Keywords:** tsunami; numerical simulation; Navier–Stokes equations; Volume of Fluid Method (VOF method); LOGOS software package



**Citation:** Kozelkov, A.; Tyatyushkina, E.; Kurulin, V.; Kurkin, A. Influence of Turbulence Effects on the Runup of Tsunami Waves on the Shore within the Framework of the Navier–Stokes Equations. *Fluids* **2022**, *7*, 117. <https://doi.org/10.3390/fluids7030117>

Academic Editors: Pengfei Xue, Fabrice Veron and Joseph J. Kuehl

Received: 9 February 2022

Accepted: 14 March 2022

Published: 20 March 2022

**Publisher's Note:** MDPI stays neutral with regard to jurisdictional claims in published maps and institutional affiliations.



**Copyright:** © 2022 by the authors. Licensee MDPI, Basel, Switzerland. This article is an open access article distributed under the terms and conditions of the Creative Commons Attribution (CC BY) license (<https://creativecommons.org/licenses/by/4.0/>).

## 1. Introduction

The Navier–Stokes equations are the most complete set of equations to describe viscous fluids, which takes into account their complex flow structure. Tsunami waves possess a number of physical properties that become evident only in the three-dimensional scenario and must be considered in their simulations. Such structures develop when the wave runs up near the shore, breaks, comes onshore, and travels overland, interacting with the coastal infrastructure. Numerical simulations of tsunami waves based on the set of three-dimensional Navier–Stokes equations [1] make it possible to explore turbulence effects during tsunami propagation and arrival on the shore, which cannot be studied by means of two-dimensional models. At present, there are a number of publications in which tsunami waves are simulated using a variety of turbulence models [2–7]. Is it really necessary to incorporate turbulence in such simulations? The issue of turbulence effects on tsunami simulations requires some additional analysis. In the models based on the nonlinear shallow-water and Boussinesq equations, turbulence is parametrized by empirical relations borrowed from the steady flow theory rather than from the wave theories, whereas turbulence is a substantial three-dimensional unsteady process [5]. Three-dimensional simulations open up the prospect of using the known and well-tested fluid turbulence models [8–15] and eddy-resolving models [16,17]. To explore the effect of turbulence on the wave as it propagates and comes onshore, in this work, we use one of the most widely used turbulence models, RANS SST [18].

In the paper, we present the results of studying the turbulence effects during tsunami propagation and runup on the shore by solving the problem of a wave propagating in

a nonuniform-bottom basin and breaking with a barrier. We describe the mathematical model, which is based on the Reynolds-averaged three-dimensional Navier–Stokes equations [11,19] and the VOF technique (Volume of Fluid Method) [20,21]. This model has been adapted for tsunami simulations [22,23]. We also describe the SST turbulence model (TM) and present the problem statement, setup the specifications, and the mesh model constructed. To assess the turbulence effects, we compare the wave profiles for each setup, calculated both with and without the use of the turbulence model. To quantify the turbulence effects, we also compare the forces acting on the basin bottom (pressure force, friction, and total force).

## 2. Mathematical Model

Let us consider a flow of substance consisting of an arbitrary number of components in different physical states. For simplicity, we assume that the components (water and air) are described by the same field of velocities and pressures, that there are no phase transitions, the components are incompressible, there are no sinks or sources, and the heat exchange processes are negligible. At this point, we ignore the effects of Earth’s rotation and sphericity. As a result, the system of Reynolds-averaged Navier–Stokes equations in the Cartesian coordinates takes the following form (the averaging signs are omitted):

$$\begin{cases} \frac{\partial}{\partial x_i}(u_i) = 0, \\ \rho \frac{\partial u_i}{\partial t} + \rho \frac{\partial}{\partial x_j}(u_i u_j) = -\frac{\partial p}{\partial x_i} + \frac{\partial}{\partial x_j}(\tau_{ij} + \tau^t_{ij}) + \rho g_i, \\ \frac{\partial \alpha_w}{\partial t} + \frac{\partial}{\partial x_i}(u_i \alpha_w) = 0, \end{cases} \quad (1)$$

where  $i, j$  are the subscripts indicating that the vector components belong to the Cartesian coordinates,  $i, j = \{x, y, z\}$ ;  $\rho$  is the mixture density calculated as  $\rho = \rho_w \alpha_w + \rho_a \alpha_a$ ;  $w$  (water) is the subscript indicating the quantities belonging to the “water” phase;  $a$  (air) is the subscript indicating the quantities belonging to the “air” phase;  $\alpha_w / \alpha_a$  is the volume fraction of water/air, respectively;  $u_i$  is the component of the velocity vector,  $i = \{x, y, z\}$ ;  $t$  is time;  $p$  is pressure;  $x_i$  is the component of the vector of the Cartesian coordinates,  $i = \{x, y, z\}$ ;  $\tau_{ij}$  is the tensor of viscous stresses, which, according to the Boussinesq hypothesis, takes the form of:

$$\tau_{ij} = \mu \left( \frac{\partial u_i}{\partial x_j} + \frac{\partial u_j}{\partial x_i} - \frac{2}{3} \frac{\partial u_k}{\partial x_k} \delta_{ij} \right),$$

$\mu_t$  is the dynamic viscosity;  $\delta_{ij}$  is the Kronecker delta; and  $g_i$  is the component of the gravitational acceleration vector.

The set of Equation (1) is not closed because we do not know how one of the basic variables in this system,  $\tau^t_{ij}$ , is related to the averaged flow parameters. This relationship, representing the contribution of turbulent fluctuations to the main flow, can be defined through some additional relations, generally referred to as turbulence models. The turbulence models are described in refs [8,9,11,16,18,19,24].

Here, we use the differential turbulence models, which employ empirical relations for the coefficient of turbulent viscosity  $\mu_t$ , the Boussinesq hypothesis, and Fourier’s law for the stress tensor:

$$\tau^t_{ij} = 2\mu_t \left( S_{ij} - \frac{1}{3} I_{ij} \nabla \cdot \vec{u} \right) + \frac{2}{3} k I_{ij}, \quad S_{ij} = \frac{1}{2} \left( \frac{\partial u_i}{\partial x_j} + \frac{\partial u_j}{\partial x_i} \right).$$

Here,  $k$  is the kinetic energy of turbulence,  $\mu_t$  is turbulent viscosity,  $I_{ij}$  is an identity matrix.

The first two equations in Equation (1) are the equations of conservation of mass and momentum, and the third one is the volume fraction transport equation of the liquid phase. For the “air” phase, the volume fraction transport equation must not be solved, because, according to the principles of the VOF method, the volume fraction  $\alpha_a$  is calculated from the relationship  $\alpha_w + \alpha_a = 1$ .

Before discretizing Equation (1), it makes sense to use transformations to improve the accuracy and stability of the solution. The momentum equation is written in a half-divergent form, because, as shown in [21], this representation compensates for the approximation errors associated with the imperfect fulfillment of the mass balance condition in the computation cells and resolves the shape of the free-surface more accurately:

$$\rho \frac{\partial u_i}{\partial t} + \frac{\partial}{\partial x_j} (u_i u_j \rho) - u_i \frac{\partial}{\partial x_j} (u_j \rho) = -\frac{\partial p}{\partial x_i} + \frac{\partial}{\partial x_j} \tau_{ij} + \rho g_i$$

Thus, the system of Equation (1) has the following final form:

$$\begin{cases} \frac{\partial u_i}{\partial x_j} = 0, \\ \rho \frac{\partial u_i}{\partial t} + \frac{\partial}{\partial x_j} (u_i u_j \rho) - u_i \frac{\partial}{\partial x_j} (u_j \rho) = -\frac{\partial p}{\partial x_i} + \frac{\partial}{\partial x_j} (\tau_{ij} + \tau^t_{ij}) + \rho g_i, \\ \frac{\partial \alpha_w}{\partial t} + \frac{\partial}{\partial x_i} (u_i \alpha_w) = 0. \end{cases} \quad (2)$$

Equation (2) enables simulations of tsunami waves, their propagation, and subsequent runup on the shore. The use of the VOF method, underlying Equation (2), allows for running numerical experiments on arbitrary geometry meshes.

To carry out the turbulence simulations, one must add some relationships to the system of Equation (2) to complete the problem. In this paper, we use for this purpose the RANS SST turbulence model, the classic formulation of which is presented in [18].

Equation (2) is discretized by the finite volume method on an arbitrary unstructured mesh and solved numerically by a fully implicit method [16,25] based on the known SIMPLE algorithm. The modeling of the free-surface flows implies some modifications of the SIMPLE algorithm developed specifically for three-dimensional tsunami simulations [22]. The basic formulations of the SIMPLE algorithm, its boundary conditions, and implementation in the LOGOS software package (a program complex for engineering analysis, focused on solving the problems of computational fluid and gas dynamics, as well as heat transfer on an arbitrary unstructured grid using parallel computing algorithms) are described in detail in [22,25,26]. This method has been widely verified, both for the free-surface problems [27] and for the problems directly associated with tsunami waves [28]. This particular form of the method has already been used to simulate historical [29] and hypothetical tsunami waves [30].

### 3. Turbulence Effects on the Wave Runup on the Shore

In order to explore turbulence effects on the propagation and transformation of a wave as it comes onshore, we simulate numerically the process of a wave traveling in a tank and collapsing with a barrier [28,31]. This problem deals with a wave moving in a tank (the wave is generated on the left boundary of the tank) having a length of 22 m and a depth of  $h_0 = 0.2$  m. The bottom of the tank has a slope starting from  $x = 10$  m and a barrier. Figure 1 shows the problem geometry.

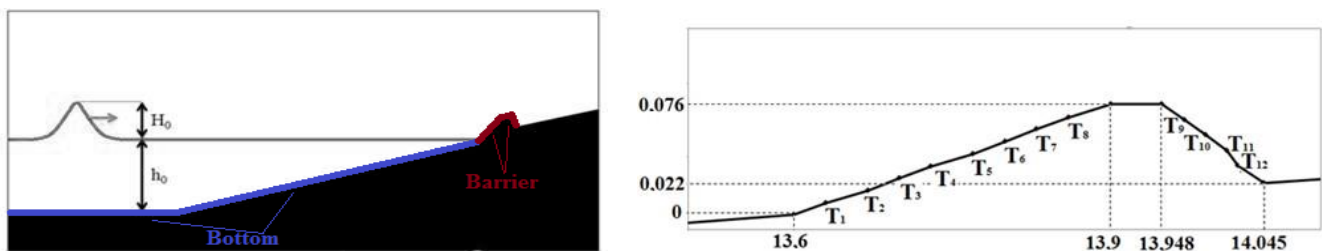


Figure 1. Schematic representation of the problem.

Elevation coordinates of the barrier are given in Table 1.

**Table 1.** Elevation coordinates of the barrier.

Point (Figure 1, Right)	Coordinates	Point (Figure 1, Right)	Coordinates	Point (Figure 1, Right)	Coordinates
$T_1$	(13.63, 0.008) m	$T_5$	(13.77, 0.042) m	$T_9$	(13.97, 0.065) m
$T_2$	(13.67, 0.017) m	$T_6$	(13.80, 0.050) m	$T_{10}$	(13.99, 0.055) m
$T_3$	(13.70, 0.025) m	$T_7$	(13.83, 0.059) m	$T_{11}$	(14.01, 0.044) m
$T_4$	(13.73, 0.033) m	$T_8$	(13.86, 0.067) m	$T_{12}$	(14.02, 0.034) m

The problem domain was discretized with a three-dimensional unstructured computational mesh consisting of truncated polyhedrons (Figure 2).

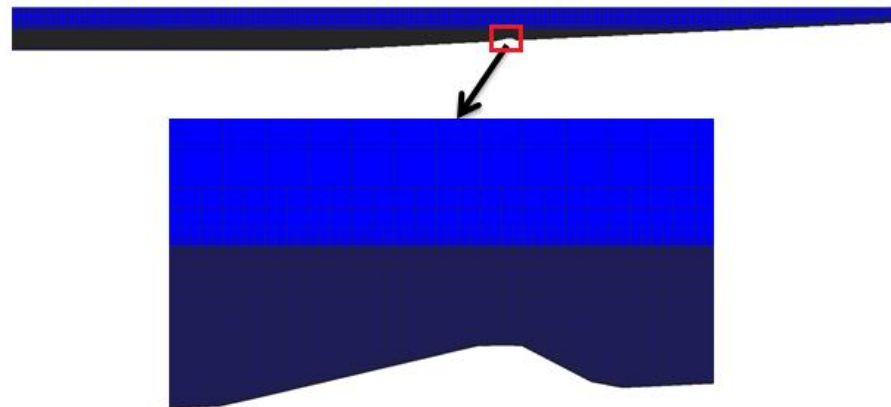


**Figure 2.** Computational mesh.

The problem was solved for different values of the Reynolds number  $Re$  (Table 2):

$$Re = \frac{\rho u L}{\mu},$$

where  $u$  is the characteristic velocity, m/s;  $L$  is the characteristic dimension, m;  $\mu$  is the dynamic viscosity, kg/(m·s).

**Table 2.** Problem setups.

Setup No.:	Reynolds Number	$H_0$ , m
1	$2.8 \times 10^4$	0.02
2	$1.92 \times 10^5$	0.07
3	$5.4 \times 10^5$	0.12
4	$7.2 \times 10^5$	0.15

The characteristic dimension  $L$ , in this problem, is represented by the undisturbed water depth (corresponding to  $h_0$  in Figure 1) and by the characteristic velocity  $u$ , the wave velocity,  $u(x, 0) = \sqrt{\frac{g}{h_0}} \eta(x, 0)$ ,  $\eta$  is the displacement of the water surface. The Reynolds number is varied by controlling the flow velocity in the wave, which in turn, is controlled by varying the wave amplitude,  $H_0$ .

The problem is simulated for two flow cases: calculation without the use of a turbulence model and calculation with the use of the SST TM.

### 3.1. Setup 1

Figure 3 shows a comparison of the wave profiles for both cases calculated using the LOGOS software package for the Reynolds number  $Re = 2.8 \times 10^4$ .

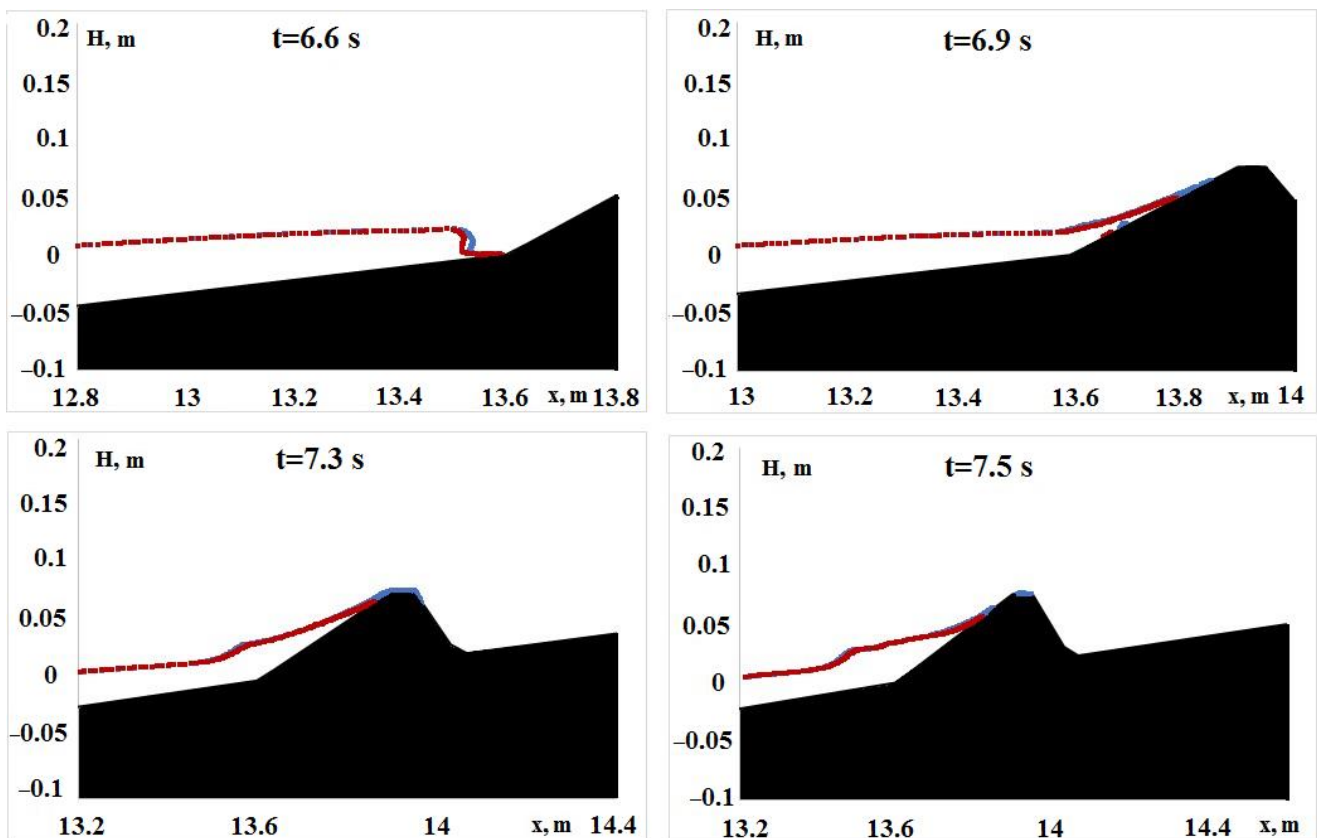


Figure 3. Comparison of the wave profiles for setup 1 (■—without TM, ■—with TM).

The subplots indicate that the wave runs up onto the barrier and then moves back. In the case without TM, the wave runs up onto the barrier at the time of 6.7 s with a small part of the fluid running over the barrier. In the same case with TM, the wave hits the barrier a little later (0.1 s) and does not run over it. This difference is explained by the fact that TM introduces additional viscosity into the solution, which represents the effect of the turbulent vortex flows and increases the viscous stress on the tank bottom, which has its effect on the runup velocity, intensity, dispersion, and nonlinear properties of the wave.

Let us present some quantitative estimates of the effect of turbulence on the propagation and runup of the wave. Figure 4 shows comparative profiles of the forces acting on the bottom. The areas on the bottom where the forces were calculated, ('Bottom'—during propagation, 'Barrier'—during runup and roll-over), are shown in Figure 1. The comparison is made for the total force  $F_s$  acting on the wall, and separately for the force of pressure  $F_p$  and the force of friction  $F_\tau$ .

The total force is defined as  $F_s = F_p + F_\tau$ , где  $F_p = p \cdot S$ ,  $p$  is the pressure acting on the surface area  $S$ ,  $F_\tau = \mu_{eff}(\partial u_i / \partial x_j)$ ,  $\mu_{eff} = \mu + \mu_t$ .

The plots show that the total force and the pressure force acting on the 'Bottom' wall in the setup with  $Re = 2.8 \cdot 10^4$  are nearly the same for both flow cases. The force of pressure in the case without TM on the 'Barrier' wall and the total force are about 5% higher than those in the case with TM, which, in our opinion, is attributed to the more active runup onto the barrier in the calculation without TM in the absence of turbulent vortex flows in the flow core. The maximum friction force is two orders higher in the calculation with TM, but the contribution of friction to the total force for this flow case is negligibly small.

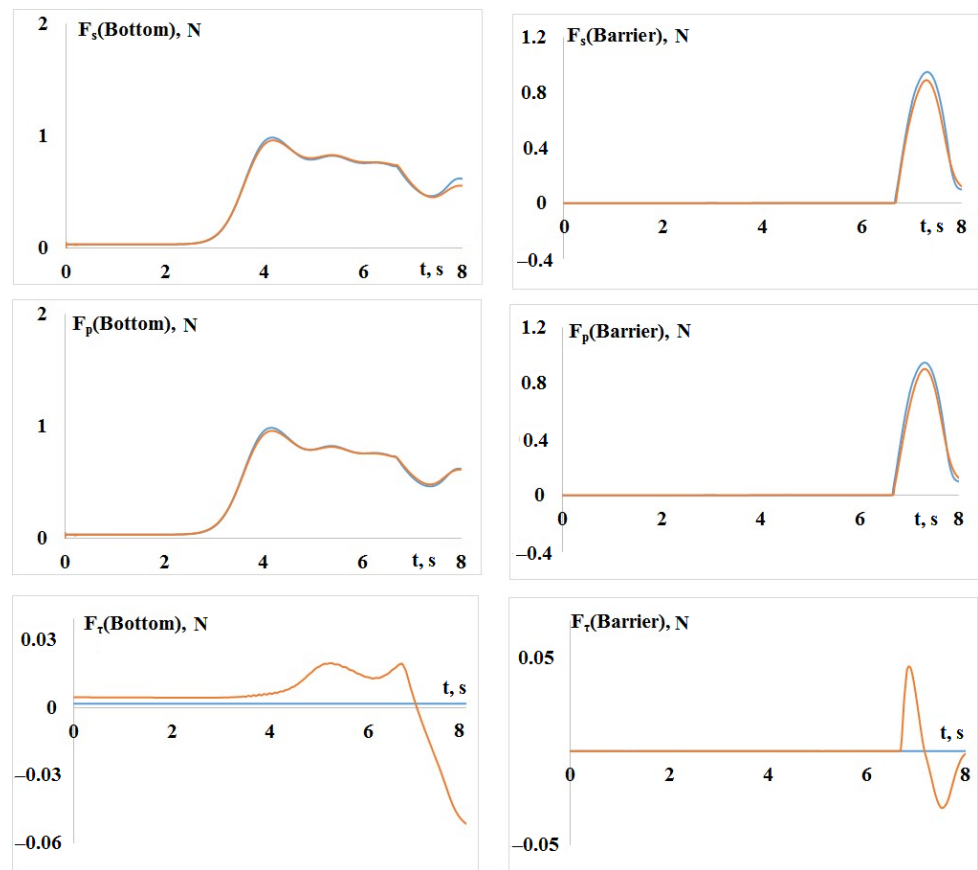


**Figure 4.** Comparison of the forces acting on the channel bottom in the slope and barrier zones (—without TM, —with TM).

### 3.2. Setup 2

Figure 5 shows a comparison of the wave profiles for both flow cases calculated by using the LOGOS software package for the Reynolds number,  $Re = 1.92 \times 10^5$ .

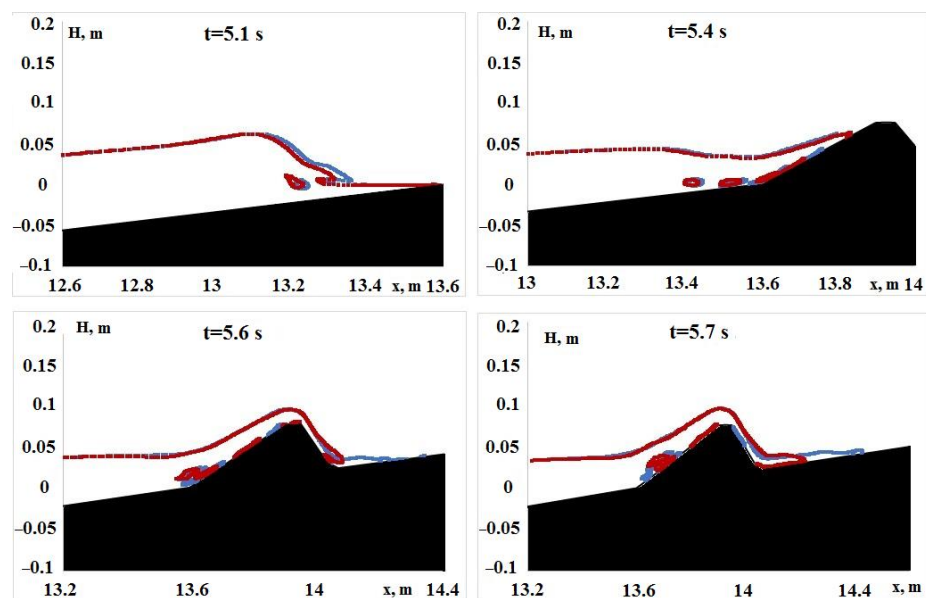


**Figure 5.** Comparison of the wave profiles for setup 2 (—without TM, —with TM).

The figures suggest that the wave in the first part of the slope first breaks and then runs up onto the barrier and flows over it. In the calculation with the turbulence model, the wave runs up onto the barrier with some delay in time. In order to explore the turbulence effects in greater detail, let us show the time series of the free-surface position and turbulent viscosity for the case with TM (Figure 6).

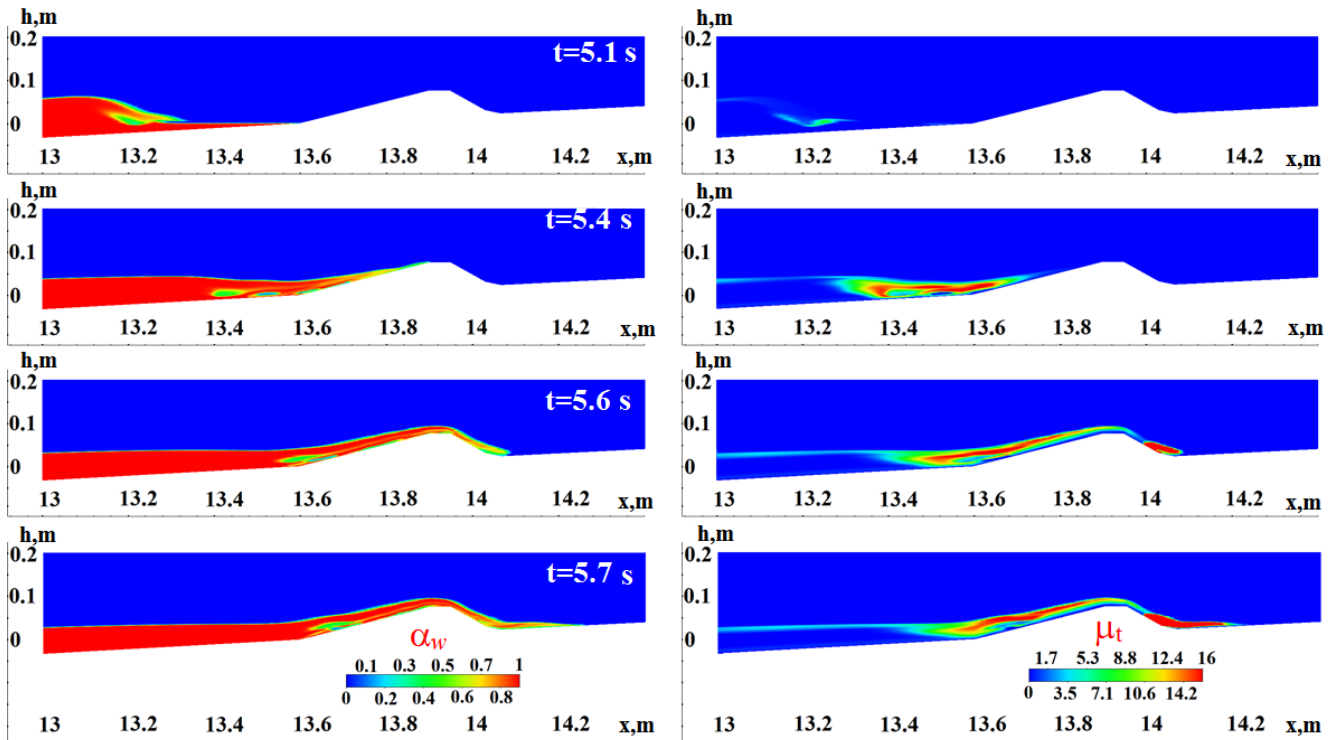


Figure 6. Time series of the free-surface position and turbulence viscosity.

The subplots show that the maximum turbulent viscosity is generated when the wave runs up and then collapses behind the barrier. The turbulent viscosity is not generated during the wave propagation, which points to the fact that TM has almost no effect at this stage.

Let us present some quantitative estimates of the effect of turbulence on the propagation and runup of the wave. Figure 7 shows comparative profiles of the forces acting on the bottom (in the slope and barrier zones) for setup 2 (Table 1). The profiles indicate that the pressure force on the ‘Bottom’ during the wave propagation in both calculations is nearly identical. One can see a peak at the time moment when the wave breaks. The friction force in the ‘Bottom’ zone in the case with TM is about 10 times higher than in the case without TM. However, its magnitude is low, and its contribution to the total force is very small.

The force of pressure acting on the ‘Barrier’ is nearly identical in both calculations. The total force in the case with TM, however, is on average 10 percent higher than in the case without TM due to the friction force.

### 3.3. Setup 3

Figure 8 shows a comparison of the wave profiles for both flow cases calculated by using the LOGOS software package for the third setup with the Reynolds number,  $Re = 5.4 \times 10^5$ .

The plots indicate that the wave runs up onto the barrier and then the fluid flows over it. In the calculation with TM, the wave runs up onto the barrier with some delay in time. In this setup, as the Reynolds number increases, one can observe more chaotic wave structures with a large number of bubbles.

Let us show the snapshots of the free-surface position and turbulent viscosity of the case with TM (Figure 9).

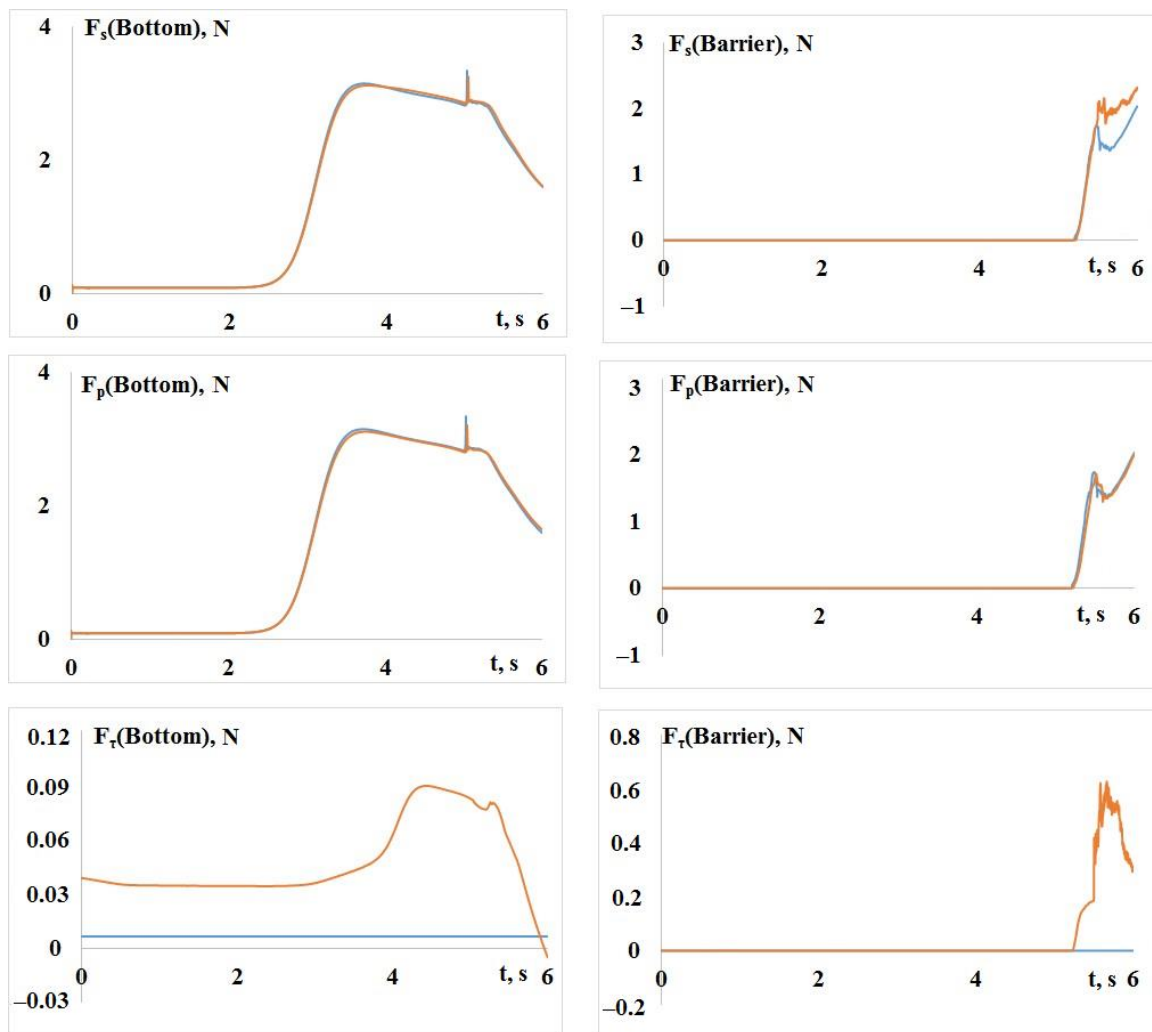


Figure 7. Comparison of the forces acting on the channel bottom in the slope and barrier zones for setup 2 (—without TM, —with TM).

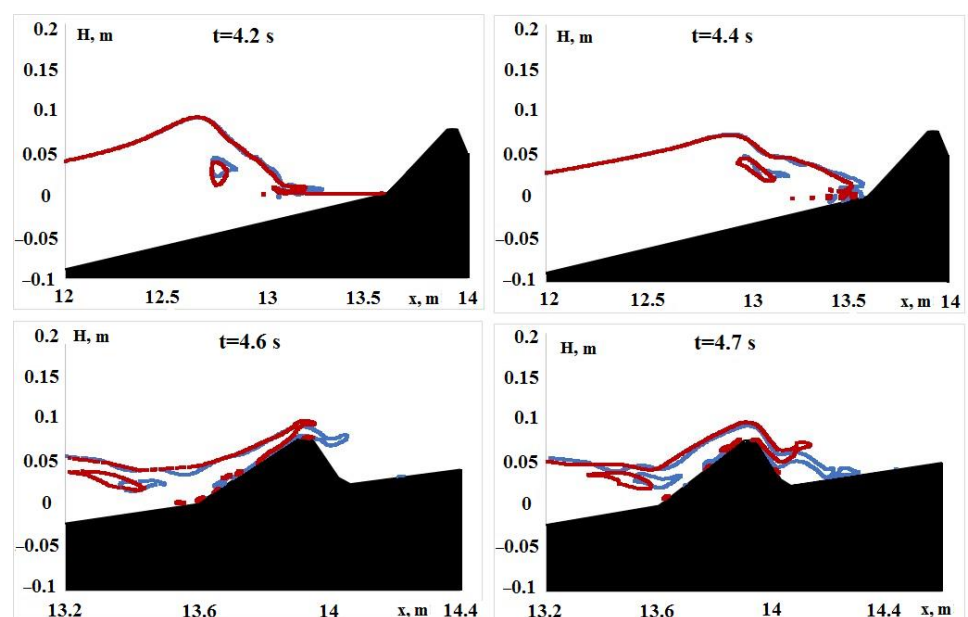


Figure 8. Comparison of the wave profiles for setup 3 (—without TM, —with TM).



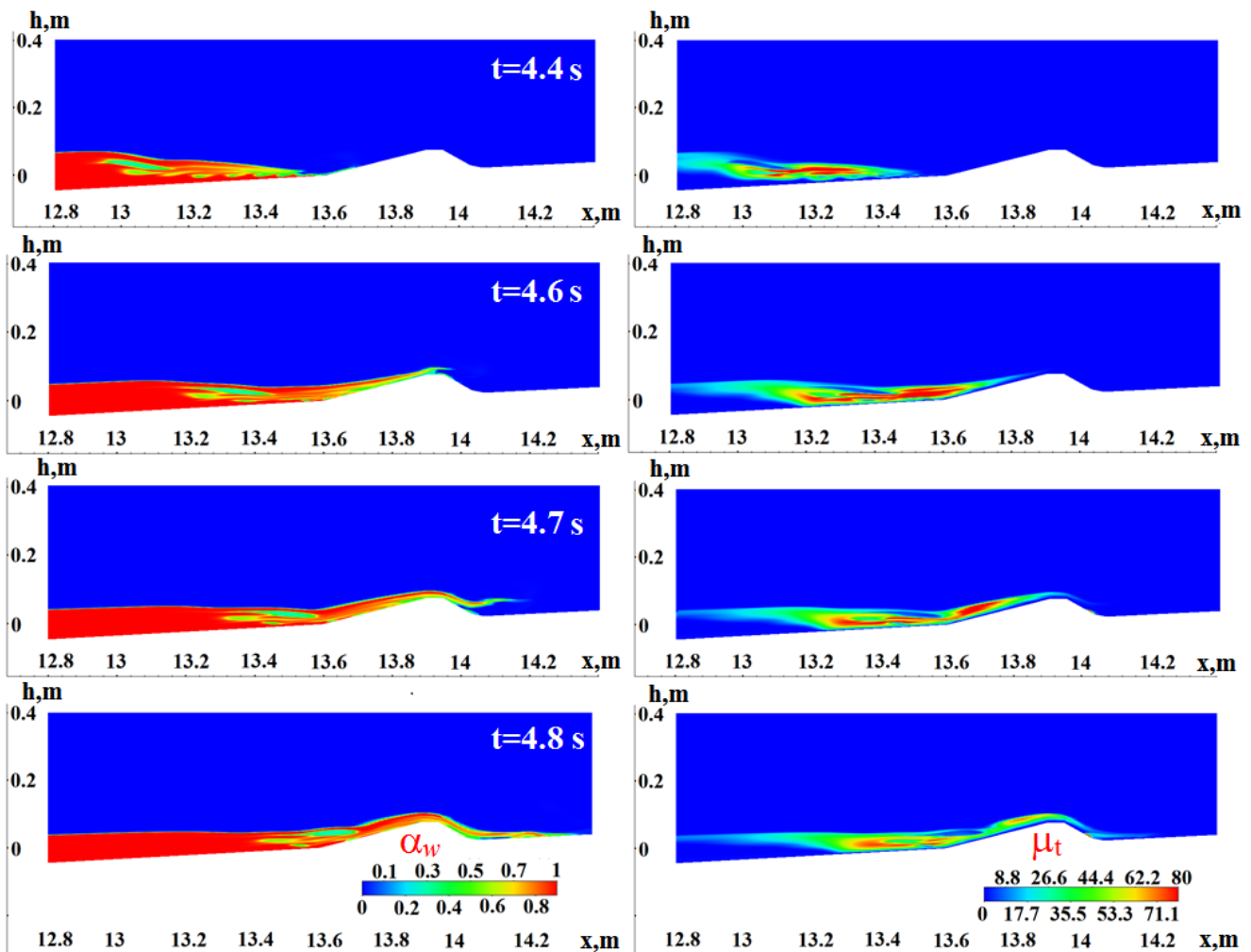


Figure 9. Time series of the free-surface position and turbulence viscosity for setup 3.

The figures show that the maximum turbulent viscosity is generated when the wave runs up and then overcomes the barrier. Let us present some quantitative estimates of the effect of turbulence on the propagation and runoff of the wave. Figure 10 shows comparative profiles of the forces acting on the bottom for setup 3.

The profiles indicate that the force of pressure acting on the ‘Bottom’ wall during the wave propagation in both calculations is nearly identical. One can see a peak at the time when the wave collapses. The difference in the magnitude of the total force in both calculations does not exceed 3%. The contribution of the friction force to the total force is very small.

The pressure force produced by the wave as it runs up onto the ‘Barrier’ zone is about 15% higher in the case with TM. The total force in the calculation with TM is about 25% higher. The total force in the case with TM is higher due to the friction force, whose contribution to the total force is about 13%.

### 3.4. Setup 4

Figure 11 shows a comparison of the wave profiles for both cases calculated using the LOGOS software package for the Reynolds number,  $Re = 7.2 \times 10^5$ .

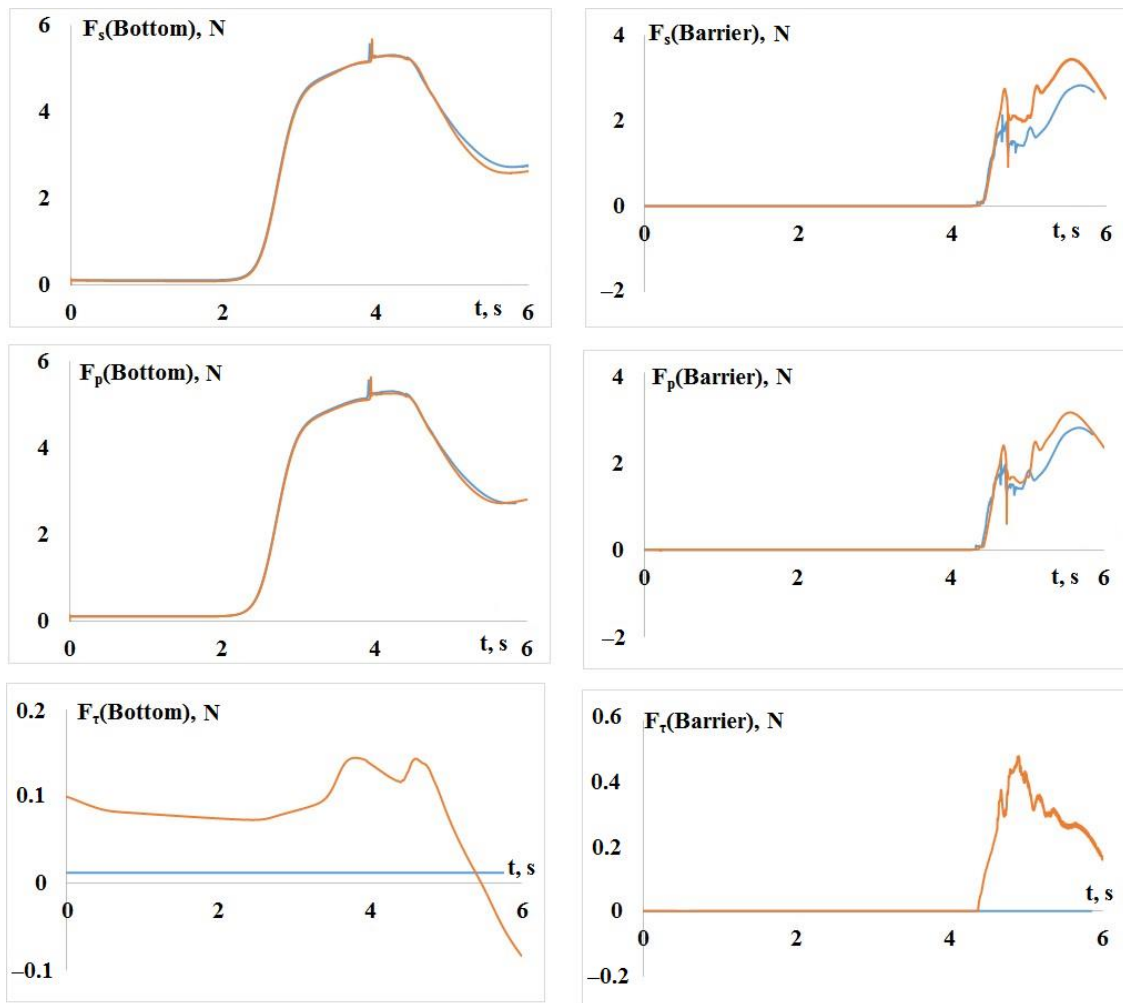


Figure 10. Comparison of the forces acting on the channel bottom in the slope and barrier zones for setup 3 (—without TM, —with TM).

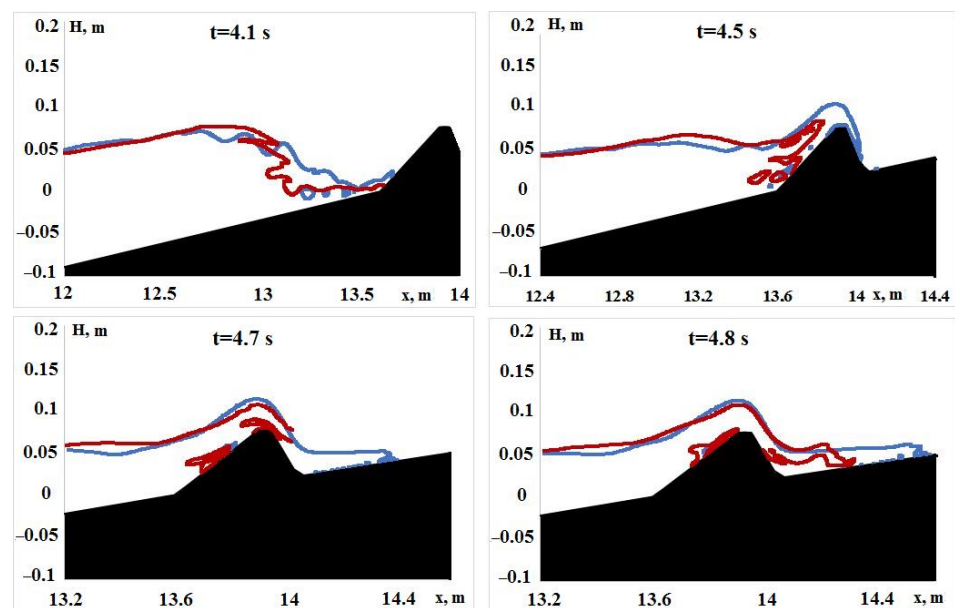


Figure 11. Comparison of the wave profiles for setup 4 (—without TM, —with TM).

The subplots indicate that the wave runs up onto the barrier and then goes over it. In the case of TM, the wave arrives with some delay in time, and, as a result, the way it overcomes the barrier is different, as shown below in the force plots.

Let us show the snapshots of the free-surface position and turbulent viscosity of the case with TM (Figure 12).

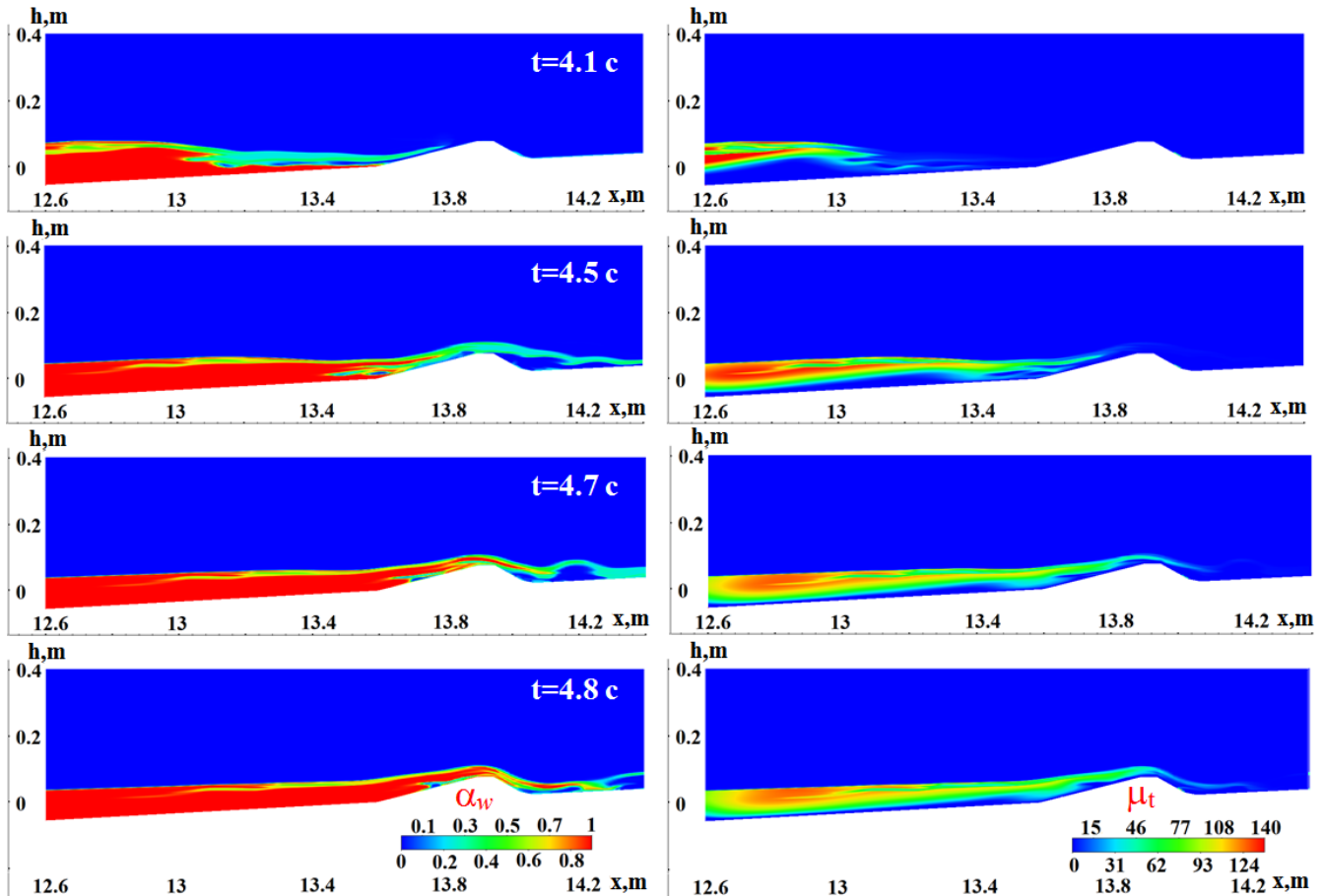


Figure 12. Time series of the free-surface position and turbulence viscosity for setup 4.

The subplots show that the maximum turbulent viscosity, in this case, is generated when the wave breaks over the slope.

Some quantitative estimates of the effect of turbulence on the propagation and runoff of the wave are presented in Figure 13, which shows comparative profiles of the forces acting on the bottom for setup 4.

The profiles indicate that the pressure force acting on the ‘Bottom’ zone during the wave propagation in both calculations is nearly identical. The difference in the magnitude of the total force in both calculations does not exceed 3%. The contribution of the friction force to the total force is very small.

The pressure force produced by the wave as it runs up onto the ‘Barrier’ is about 10% higher in the case with TM. On average, the total force in the calculation is 18% higher. The total force in the case with TM is higher due to the force of friction, the contribution of which to the total force is about 8%.

Generally speaking, the presented results and quantitative estimates of the forces of friction and pressure and the total force acting on the channel bottom suggest that turbulence has almost no effect on the shape and way of propagation in the phase of wave propagation (without breaking). However, turbulence effects during the runup and breaking become noticeable and can boost the flow (increase the force of its pressure and the total force) by up to 25%.

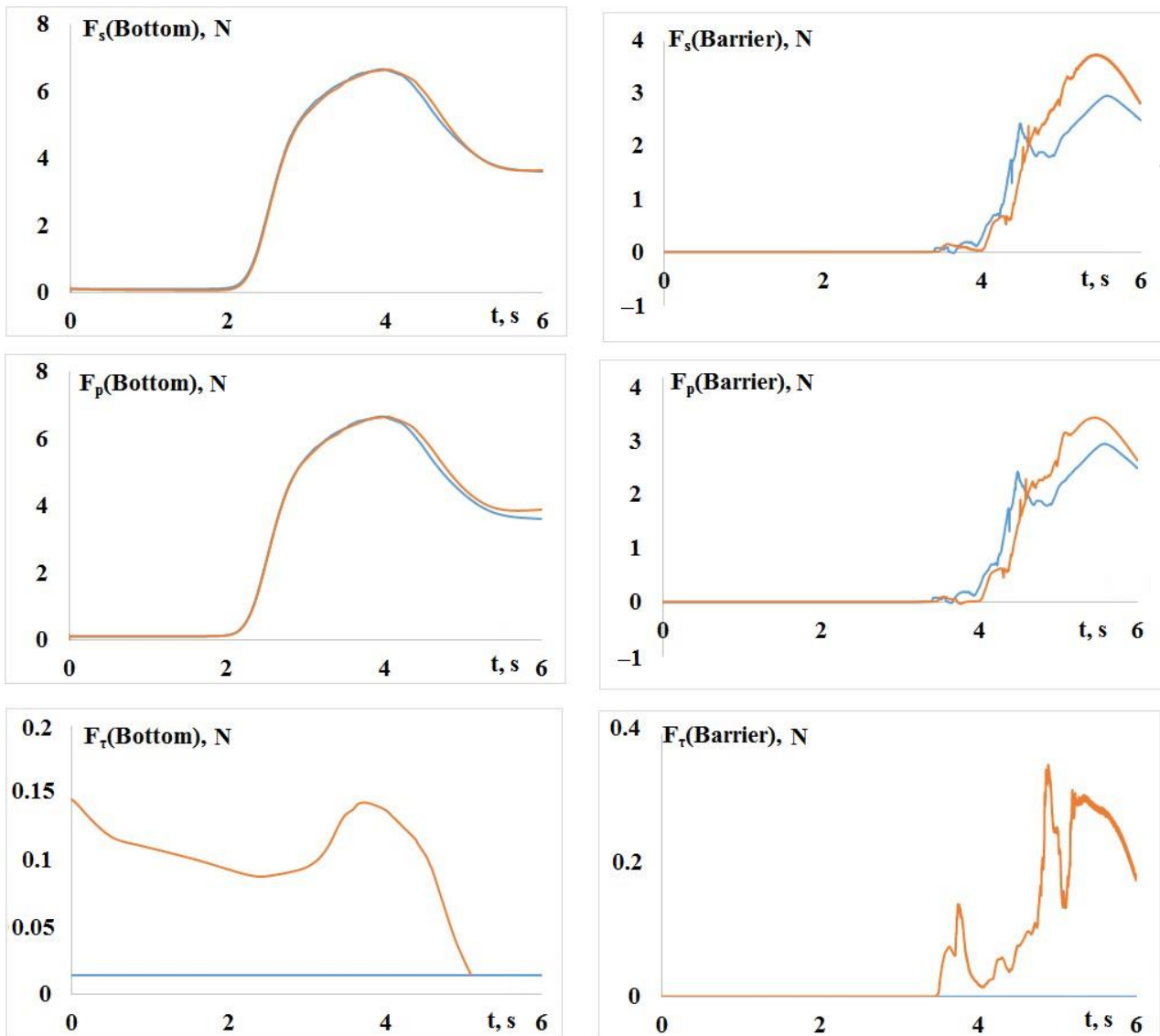


**Figure 13.** Comparison of the forces acting on the channel bottom in the slope and barrier zones for setup 4 (—without TM, —with TM).

#### 4. Conclusions

The paper provides a description of wave transformation and its interaction with an inclined bottom and a barrier. It is demonstrated within the mathematical model based on the three-dimensional Navier–Stokes equations, the VOF method, and the RANS SST turbulence model. The turbulence effects in the phases of wave propagation and runup are studied. We compare the wave profiles at different times during wave propagation, runup, and collapse. The wave profiles are compared for the cases with and without TM. We demonstrate that, in the case with TM, the wave runs up onto the barrier a little later. The use of TM introduces additional viscosity into the solution, which represents the effect of turbulent vortex flows and increases the viscous stress on the tank bottom, which has its effect on the runup velocity, intensity, dispersion, and nonlinear properties of the wave. We show that turbulence has almost no effect on the shape of the wave and the way of its propagation (except the breaking itself). Turbulence effects during the runup and breaking, however, become noticeable and can boost the flow (increase the force of its pressure and the total force) by up to 25%.

**Author Contributions:** Conceptualization, A.K. (Andrey Kozelkov ) and A.K. (Andrey Kurkin); data curation, E.T. and V.K.; formal analysis, A.K. (Andrey Kozelkov) and V.K.; investigation, E.T., A.K. (Andrey Kozelkov), A.K. (Andrey Kurkin) and V.K.; methodology, A.K. (Andrey Kozelkov), A.K. (Andrey Kurkin) and V.K.; software, E.T. and V.K.; supervision, A.K. (Andrey Kurkin); validation, E.T.; visualization, E.T.; writing—original draft, A.K. (Andrey Kozelkov) and A.K. (Andrey Kurkin) . All authors have read and agreed to the published version of the manuscript.

**Funding:** The reported study was funded by the Ministry of Science and Higher Education of the Russian Federation (project No. FSWE-2021-0009) and the Council of the grants of the President of the Russian Federation for the state support of Leading Scientific Schools of the Russian Federation (Grant No. NSH-70.2022.1.5).

**Conflicts of Interest:** The authors declare no conflict of interest.

## References

- Landau, L.D.; Lifshitz, E.M. *Fluid Mechanics: V. 6*; Elsevier: Amsterdam, The Netherlands, 2013; p. 558.
- Kim, D.C.; Kim, K.O.; Pelinovsky, E.N.; Didenkulova, I.I.; Choi, B.H. Three-dimensional tsunami runup simulation for the port of Koborinai on the Sanriku coast of Japan. *J. Coast. Res.* **2013**, *65*, 266–271. [[CrossRef](#)]
- Yuk, D.; Yim, S.C.; Liu, P.L.-F. Numerical modeling of submarine mass-movement generated waves using RANS model. *Comput. Geosci.* **2006**, *32*, 927–935. [[CrossRef](#)]
- Zhao, Q.; Armfield, S.; Tanimoto, K. Numerical simulation of breaking waves by a multi-scale turbulence model. *Coast. Eng.* **2004**, *51*, 53–80. [[CrossRef](#)]
- Choi, B.H.; Kim, D.C.; Pelinovsky, E.; Woo, S.B. Three-dimensional simulation of tsunami run-up around conical island. *Coast. Eng.* **2007**, *54*, 618–629. [[CrossRef](#)]
- Pelinovsky, E.; Choi, B.H.; Talipova, T.; Woo, S.B.; Kim, D.C. Solitary wave transformation on the underwater step: Asymptotic theory and numerical experiments. *Appl. Math. Comput.* **2010**, *217*, 1704–1718. [[CrossRef](#)]
- Choi, B.H.; Pelinovsky, E.; Kim, D.C.; Didenkulova, I.; Woo, S.-B. Two- and three-dimensional computation of solitary wave runup on non-plane beach. *Nonlinear Processes Geophys.* **2008**, *15*, 489–502. [[CrossRef](#)]
- Garbaruk, A.V.; Strelets, M.K.; Travin, A.K.; Shur, M.L. *Up-to-Date Approaches to Turbulence Simulations: A Study Guide*; Publishing House of Peter the Great St./Petersburg Polytechnic University: Saint Petersburg, Russia, 2016; p. 233.
- Volkov, K.N.; Emelyanov, V.N. *Large Eddy Simulations in Calculations of Turbulent Flows*; Fizmatlit: Moscow, Russia, 2008; p. 368.
- Belov, I.A.; Isaev, S.A. *Simulations of Turbulent Flows: A Study Guide*; Publishing House of Baltic State Technical University: Saint Petersburg, Russia, 2001; p. 108.
- Lesieur, M. *Turbulence in Fluids*, 4th ed.; Springer: Dordrecht, The Netherlands, 2008; p. 558.
- Tanaka, H.; Tinh, N.X.; Sana, A. Transitional Behavior of a Flow Regime in Shoaling Tsunami Boundary Layers. *J. Mar. Sci. Eng.* **2020**, *8*, 700. [[CrossRef](#)]
- Sana, A.; Tanaka, H. Numerical modeling of a turbulent bottom boundary layer under solitary waves on a smooth surface. *Coast. Eng. Proc.* **2018**, *36*, 152266. [[CrossRef](#)]
- Tinh, N.X.; Tanaka, H. Study on boundary layer development and bottom shear stress beneath a tsunami. *Coast. Eng. J.* **2019**, *61*, 574–589. [[CrossRef](#)]
- Sana, A.; Tanaka, H. Two-equation turbulence modeling of an oscillatory boundary layer under steep pressure gradient. *Can. J. Civ. Eng.* **2010**, *37*, 648–656. [[CrossRef](#)]
- Kozelkov, A.S.; Kurulin, V.V.; Tyatyushkina, E.S.; Puchkova, O.L. Application of the detached-eddy simulation model for viscous incompressible turbulent flow simulations on unstructured grids. *Math. Models Comput. Simul.* **2014**, *26*, 81–96.
- Kozelkov, A.; Kurulin, V.; Emelyanov, V.; Tyatyushkina, E.; Volkov, K. Comparison of convective flux discretization schemes in detached-eddy simulation of turbulent flows on unstructured meshes. *J. Sci. Comput.* **2016**, *67*, 176–191. [[CrossRef](#)]
- Menter, F.R.; Kuntz, M.; Langtry, R. Ten Years of Industrial Experience with the SST Turbulence Model. In *Turbulence, Heat and Mass Transfer*, 4th ed.; Hanjalic, K., Nagano, Y., Tummers, M., Eds.; Begell House Inc.: Danbury, CT, USA, 2003; pp. 625–632.
- Zaikov, L.A.; Strelets, M.K.; Shur, M.L. A comparison between one- and two-equation differential turbulence models in application to separated and attached flows: Flow in channels with counter. *High Temp.* **1996**, *34*, 713–725.
- Ubbink, O. Numerical Prediction of Two Fluid Systems with Sharp Interfaces. Ph.D. Thesis, Imperial College of Science, Technology & Medicine, London, UK, 1997.
- Khrabry, A.I.; Zaytsev, D.K.; Smirnov, E.M. Numerical simulations of free-surface flows based on the VOF method. *Trans. Krylov State Res. Cent.* **2003**, *78*, 53–64.
- Kozelkov, A.S. The Numerical Technique for the Landslide Tsunami Simulations Based on Navier-Stokes Equations. *J. Appl. Mech. Tech. Phys.* **2017**, *58*, 1192–1210. [[CrossRef](#)]
- Kozelkov, A.S.; Efremov, V.R.; Kurkin, A.A.; Pelinovsky, E.N.; Tarasova, N.V.; Strelets, D.Y. Three dimensional numerical simulation of tsunami waves based on the Navier-Stokes equations. *Sci. Tsunami Hazards* **2017**, *36*, 183–196.

24. Kozelkov, A.S.; Kurulin, V.V.; Lashkin, S.V.; Shagaliev, R.M.; Yalozo, A.V. Investigation of supercomputer capabilities for the scalable numerical simulation of computational fluid dynamics problems in industrial applications. *Comput. Math. Math. Phys.* **2016**, *56*, 1506–1516. [[CrossRef](#)]
25. Chen, Z.J.; Przekwas, A.J. A coupled pressure-based computational method for incompressible/compressible flows. *J. Comput. Phys.* **2010**, *229*, 9150–9165. [[CrossRef](#)]
26. Kozelkov, A.S.; Lashkin, S.V.; Efremov, V.R.; Volkov, K.N.; Tsibereva, Y.A.; Tarasova, N.V. An implicit algorithm of solving Navier–Stokes equations to simulate flows in anisotropic porous media. *Comput. Fluids* **2018**, *160*, 164–174. [[CrossRef](#)]
27. Kozelkov, A.S.; Kurkin, A.A.; Sharipova, I.L.; Kurulin, V.V.; Pelinovsky, E.N.; Tyatyushkina, E.S.; Meleshkina, D.P.; Lashkin, S.V.; Tarasova, N.V. A minimum basic set of validation problems for free-surface flow simulation methods. *Trans. NNSTU N.A. R.E. Alekseev.* **2015**, *2*, 49–69.
28. Tyatyushkina, E.S.; Kozelkov, A.S.; Kurkin, A.A.; Pelinovsky, E.N.; Kurulin, V.V.; Plygunova, K.S.; Utkin, D.A. Verification of the LOGOS Software Package for Tsunami Simulations. *Geosciences* **2020**, *10*, 385. [[CrossRef](#)]
29. Kozelkov, A.S.; Kurkin, A.A.; Pelinovsky, E.N.; Kurulin, V.V.; Tyatyushkina, E.S. Modeling the Disturbances in the Lake Chebarkul Caused by the Fall of the Meteorite in 2013. *Fluid Dyn.* **2015**, *50*, 828–840. [[CrossRef](#)]
30. Kozelkov, A.S.; Kurkin, A.A.; Pelinovsky, E.N.; Kurulin, V.V. Modeling the cosmogenic tsunami within the framework of the Navier-Stokes equations with sources of different type. *Fluid Dyn.* **2015**, *50*, 306–313. [[CrossRef](#)]
31. Hsiao, S.-C.; Lin, T.-C. Tsunami-like solitary waves impinging and overtopping an impermeable seawall: Experiment and RANS modeling. *Coast. Eng.* **2010**, *57*, 1–18. [[CrossRef](#)]